JOURNAL OF
THE ENGINEERING
MECHANICS DIVISION

# RESPONSE OF LAYER TO STRIKE-SLIP VERTICAL FAULT

By Marijan Dravinski[1] and Mihailo D. Trifunac,[2] M. ASCE

## INTRODUCTION

The problem presented in this paper represents a special case of the model studied by the writers in Ref. 2, in which they evaluated response of a multilayered medium subjected to a vertical strike-slip fault and analyzed its application to earthquake engineering and geophysics.

The purpose of this paper is to present a different method of solution and to illustrate the nature of the results in the case of single elastic layer overlying the rigid half space. Though too simple for many practical applications, this model can serve as a test case for more general numerical models in earthquake engineering and strong motion seismology dealing with strong shaking in the near field. The exact analytical solution presented here can thus be employed to critically examine the quality of the approximate boundary conditions, mesh size, and integration schemes in Finite Element and Finite Difference approximations that deal with similar and related problems (2). The results of this analysis can further be employed to better understand the physical nature of the near field strong shaking in the vicinity of a vertical strike-slip fault in detail which is possible only in terms of the exact analytical solution.

This paper presents only the solution to the steady-state periodic source, since it contains all relevant physical characteristics of the problem. Through Fourier synthesis (2), it is possible to construct the details of transient motion everywhere in the model.

Note.—Discussion open until January 1, 1981. To extend the closing date one month, a written request must be filed with the Manager of Technical and Professional Publications, ASCE. This paper is part of the copyrighted Journal of the Engineering Mechanics Division, Proceedings of the American Society of Civil Engineers, Vol. 106, No. EM4, August, 1980. Manuscript was submitted for review for possible publication on August 14, 1979.

[1]Research Assoc., Dept. of Civ. Engrg., Univ. of Southern California, Los Angeles, Calif.

[2]Prof., Dept. of Civ. Engrg., Univ. of Southern California, Los Angeles, Calif.

## STATEMENT OF PROBLEM

The model shown in Fig. 1 consists of a homogeneous, isotropic, linearly elastic layer which extends to infinity along the $y$-axis. The layer is bonded to a rigid half-space and subjected to a prescribed antisymmetric displacement field at $x = 0$ uniformly along the $y$-axis. The problem just presented is the antiplane-strain type in which the displacement field is given by $u_x = u_z = 0$ and $u_y = v(x, z, t)$, in which the subscripts on $u_x$, $u_y$ and $u_z$ denote components of the displacement vector along the coordinate axes $x$, $y$, and $z$, respectively. The steady-state displacement input is defined by

$$v^i = v(x = 0^+, z, \omega) = g(z) F(\omega) e^{-i\omega t} \quad \ldots \ldots \ldots \ldots \ldots \ldots \ldots \ldots \quad (1)$$

with functions $g(z)$ and $f(\omega)$ being known.

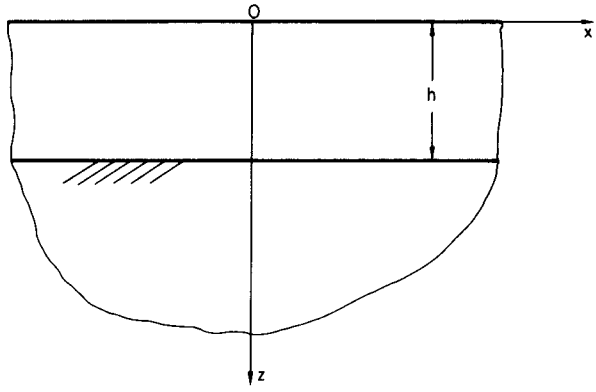


**FIG. 1.—Model Geometry**

The equation of motion is given by

$$\left[\nabla^2 + \frac{\omega^2}{\beta^2}\right] v(x, z, \omega) = 0; \quad \nabla^2 \equiv \frac{\partial^2}{\partial x^2} + \frac{\partial^2}{\partial z^2}; \quad x \in (-\infty, \infty); \quad z \in [0, h] \qquad (2)$$

in which $\beta$ = the shear wave velocity of the layer; $\omega$ = the circular frequency; and $h$ = the thickness of the layer. By symmetry of the model and antisymmetric excitation at $x = 0$, the resulting wave motion becomes antisymmetric with respect to $x = 0$. Thus, it is sufficient to study the motions for $x \geq 0$ only.

The top surface of the layer is stress-free and the bottom surface is perfectly bonded to a rigid half space; therefore, the boundary conditions are specified through

$$\frac{\partial v(x, 0, \omega)}{\partial z} = 0 \quad \ldots \ldots \ldots \ldots \ldots \ldots \ldots \ldots \ldots \ldots \ldots \ldots \quad (3)$$

$$v(x, h, 0) = 0 \quad \ldots \ldots \ldots \ldots \ldots \ldots \ldots \ldots \ldots \ldots \ldots \ldots \quad (4)$$

**Solution of Problem**

Since the wave motion is antisymmetric in $x$, the sine Fourier transform is introduced, defined by a pair (5)

$$\tilde{f}(\xi) = 2\int_0^\infty f(x)\sin\xi x\,dx \quad \ldots\ldots\ldots\ldots\ldots\ldots\ldots\ldots\ldots\ldots\ldots\ldots (5)$$

$$f(x) = \frac{1}{\pi}\int_0^\infty f(\omega)\sin\xi x\,d\xi \quad \ldots\ldots\ldots\ldots\ldots\ldots\ldots\ldots\ldots\ldots\ldots\ldots (6)$$

Application of the sine Fourier transform of Eq. 2 implies

$$\left[\frac{\partial^2}{\partial z^2} + \left(\frac{\omega^2}{\beta^2} - \xi^2\right)\right]\tilde{v}(\xi, z, \omega) = 2\xi g(z) f(\omega) \quad \ldots\ldots\ldots\ldots\ldots\ldots\ldots\ldots (7)$$

By extending the displacement field first as an odd function about $z = h$ in the region $h \le z \le 2h$, and then as an even function with respect to $z = 0$ over an interval $-2h \le z \le 0$, it follows that

$$\frac{\partial\,\tilde{v}(\xi, 0, \omega)}{\partial z} = \frac{\partial\,\tilde{v}(\xi, 2h, \omega)}{\partial z} = 0 \quad \ldots\ldots\ldots\ldots\ldots\ldots\ldots\ldots\ldots\ldots\ldots\ldots (8)$$

The last property calls for application of the finite cosine transform defined by a pair

$$\tilde{v}^*(\xi, n, \omega) = \int_0^{2h} \tilde{v}(\xi, z, \omega)\cos\frac{n\pi z}{2h}\,dz \quad \ldots\ldots\ldots\ldots\ldots\ldots\ldots\ldots\ldots\ldots (9)$$

$$\tilde{v}(\xi, z, \omega) = \frac{1}{2h}\,v^*(\xi, 0, \omega) + \frac{1}{h}\sum_{n=1}^{\infty}\tilde{v}^*(\xi, n, \omega)\cos\frac{n\pi z}{2h} \quad \ldots\ldots\ldots\ldots\ldots\ldots\ldots\ldots (10)$$

Application of the finite cosine transform to Eq. 7 yields

$$\tilde{v}^*(\xi, n, \omega) = \frac{2\xi F(\omega)}{q^2 - \left(\frac{n\pi}{2h}\right)^2} b_n; \quad n = 1, 2, 3, \ldots \quad \ldots\ldots\ldots\ldots\ldots\ldots\ldots\ldots\ldots\ldots (11)$$

in which $q^2 = \dfrac{\omega^2}{\beta^2} - \xi^2$ $\ldots\ldots\ldots\ldots\ldots\ldots\ldots\ldots\ldots\ldots\ldots\ldots\ldots\ldots\ldots\ldots\ldots\ldots\ldots\ldots (12)$

$$b_n = \int_0^{2h} g(\zeta)\cos\frac{n\pi\zeta}{2h}\,d\zeta \quad \ldots\ldots\ldots\ldots\ldots\ldots\ldots\ldots\ldots\ldots\ldots\ldots\ldots\ldots\ldots\ldots\ldots\ldots\ldots\ldots (13)$$

Inversion of the finite cosine transform implies

$$\tilde{v}(\xi, z, \omega) = -\frac{2F(\omega)}{h}\sum_{m=1}^{\infty}\frac{\xi}{q^2 - \left(\frac{n\pi}{2h}\right)^2} b_n \cos\frac{n\pi}{2h}\,z \quad \ldots\ldots\ldots\ldots\ldots\ldots\ldots\ldots\ldots\ldots\ldots\ldots (14)$$

To satisfy the remaining boundary condition in Eq. 4, the displacement field $\tilde{v}(\xi, z, \omega)$ is written in the following form

$$\bar{v}(\xi, z, \omega) = -\frac{2F(\omega)}{h} \sum_{m=1}^{\infty} \frac{\xi}{q^2 - \left[\frac{(2m-1)\pi}{2h}\right]^2} b_{2m-1} \cos \frac{(2m-1)\pi}{2h} z \qquad (15)$$

Inversion of this cosine integral transform then gives the displacement field as

$$v(x, z, \omega) = -\frac{2F(\omega)}{h} \sum_{n=1}^{\infty} b_{2m-1} \left[\cos \frac{(2m-1)\pi}{2h} z\right]$$

$$\int_0^{\infty} \frac{\xi \sin \xi x}{q^2 - \left[\frac{(2m-1)\pi}{2h}\right]^2} d\xi \qquad (16)$$

The $\xi$-integral is evaluated next by considering the following integral in complex $\xi$-plane.

$$I = \int_{-\infty}^{\infty} \frac{\xi e^{i\xi x}}{q^2 - \left[\frac{(2m-1)\pi}{2h}\right]^2} d\xi \qquad (17)$$

The simple poles of the integral are determined by

$$\frac{\omega^2}{\beta^2} - \xi_m^2 = \left[\frac{(2m-1)\pi}{2h}\right]^2; \quad m = 1, 2, 3, \ldots \qquad (18)$$

Eq. 18 is recognized as a frequency equation for the problem under consideration (1). Assuming at a given frequency $\omega$ that

$$\xi_m^2 > 0; \quad m \geq n \qquad (19)$$

$$\xi_m^2 < 0; \quad m < n \qquad (20)$$

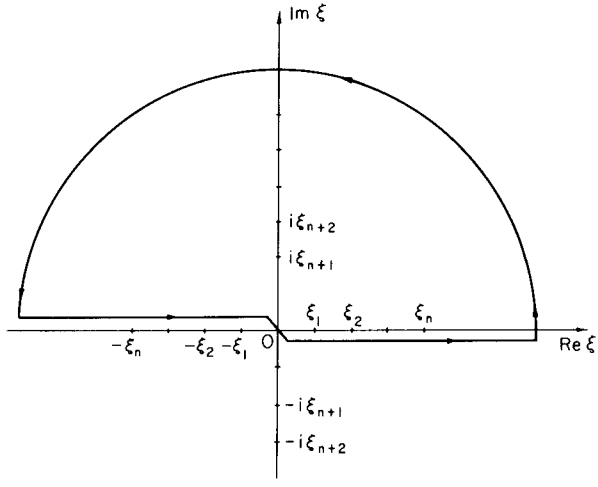


**FIG. 2.—Contour Integration and Poles in Complex $\xi$-Plane**

the poles for the integral in Eq. 17 are depicted by Fig. 2. Since the waves moving to the right (and $x > 0$) are of interest only, the proper contour of integration is shown by Fig. 2. An application of Jordan's lemma (2) leads to the result

$$\int_0^\infty \frac{\xi \sin \xi x}{q^2 - \left[\frac{(2m-1)\pi}{2h}\right]^2} d\xi = -\frac{\pi}{2}\left(\sum_{m+1}^{n} e^{i\xi_m x} + \sum_{m=n+1}^{\infty} e^{-\xi_m x}\right) \quad \ldots\ldots (21)$$

Consequently, the displacement field is given by

$$v(x, z, \omega) = \frac{F(\omega)}{h}\left\{\sum_{m=1}^{n} b_{2m-1} \cos \frac{(2m-1)\pi z}{2h} e^{i\xi_m x} + \sum_{m=n+1}^{\infty} b_{2m-1} \cos \frac{(2m-1)\pi z}{2h} e^{-\xi_m x}\right\} e^{-i\omega t} \quad \ldots\ldots (22)$$

Examination of this displacement field shows that real poles, $\xi_m^2 > 0$, correspond to progressing waves, while the pure imaginary poles, $\xi_m^2 < 0$, imply locally standing waves. Therefore, motion of the layer at a frequency $\omega$ consists of the superposition of a finite number of progressing modes and an infinite number of locally standing modes.

### Dispersion Relation

Frequency Eq. 18 can be written in dimensionless form (1,3)

$$\Omega^2 - \kappa_m^2 = \left[\frac{(2m-1)\pi}{2}\right]^2; \quad m = 1, 2, \ldots, \infty \quad \ldots\ldots (23)$$

The dimensionless frequency $\Omega$ and wave number $\kappa_m$ are defined by

$$\Omega \equiv \frac{\omega h}{\beta} \quad \ldots\ldots (24)$$

$$\kappa_m \equiv \xi_m h \quad \ldots\ldots (25)$$

For the real wave numbers, the frequency equation reduces to the family of hyperbolae; for the pure imaginary waves numbers, it reduces to the family of circles (1). This dispersion relation is depicted by Fig. 3. Analysis of Fig. 3 reveals a change in the number of progressing modes with an increase of frequency. Below the cutoff frequency, $\Omega < \pi/2$, an infinite number of locally standing modes are excited in the system (there are no progressing modes). For the frequency $\Omega > \pi/2$, in addition to an infinite number of locally standing modes, there exists a finite number of progressing modes. This fact is reflected in the structure of the displacement field in Eq. 22.

Because of the exponential decay of locally standing modes with distance $x$ from the source, their contribution is of interest in the near field only. In the far field, the displacement field due to locally standing waves may be neglected.

## Evaluation of Results

To illustrate the preceding results, the input field (Eq. 4) is assumed to be of the following form (2)

$$g(z) = v_o[H(z-\tau h) - H(z-\eta h)]; \quad 0 \le z \le h,\ 0 < \tau,\ \eta < 1,\ \tau < \eta \quad \ldots \quad (26)$$

$$F(\omega) = \int_{-\infty}^{\infty} f(t)e^{i\omega t}\,dt = \frac{a}{t_o}\frac{e^{i\omega t_o} - 1}{\omega^2} + \zeta a \frac{2\pi}{t_o}\frac{e^{i\omega t_o}}{\omega^2 - \left(\frac{2\pi}{t_o}\right)^2} \quad \ldots \quad (27)$$

in which $f(t) = f_1(t) + f_2(t)$ . . . . . (28)

$$f_1(t) = \frac{a}{t_o}t, \quad 0 \le t \le t_o; \quad f_1(t) = a, \quad t > t_o; \quad f_1(t) = 0, \quad t < 0 \quad \ldots \quad (29)$$

$$f_2(t) = \zeta a \sin\frac{2\pi}{t_o}t; \quad 0 \le t \le t_o; \quad f_2(t) = 0, \quad t_o < t < 0, \quad 0 < \zeta < 1 \quad \ldots \quad (30)$$

and $H$ represents the Heaviside step function. These input functions describe

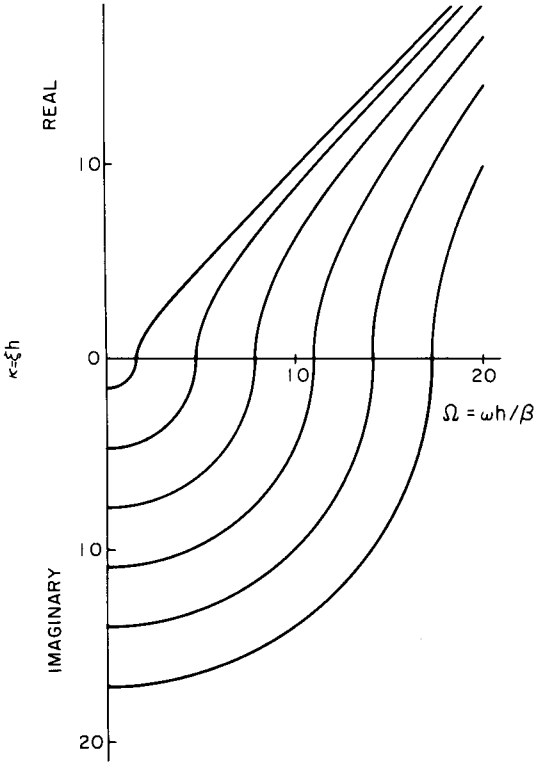


**FIG. 3.—Dispersion Curves for $h$ = 1 m, $\beta$ = 1 m/s**

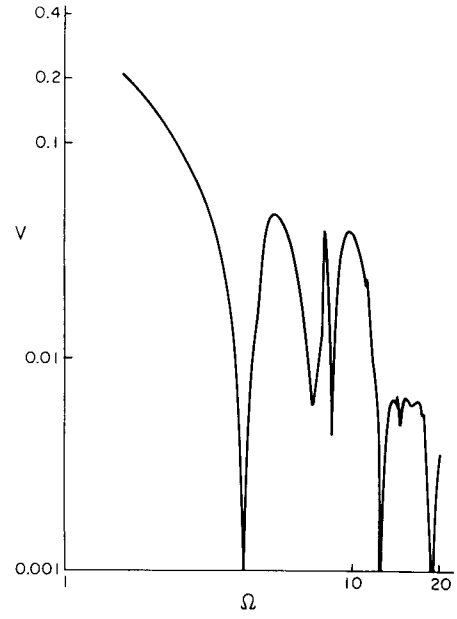


**FIG. 4.—Progressing Waves: Frequency Amplitude Spectrum for Shallow Source ($\tau = 0$, $\eta = 0.2$, $\beta = 1$ m/s, $h = 1$ m)**

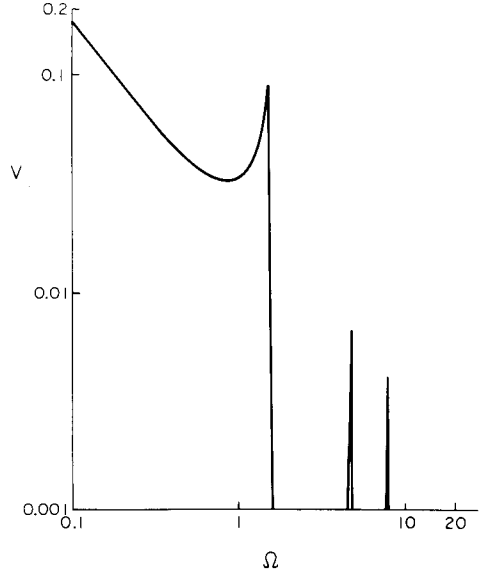


**FIG. 5.—Locally Standing Waves: Frequency Amplitude Spectrum for Shallow Source ($\tau = 0$, $\eta = 0.2$, $\beta = 1$ m/s, $h = 1$ m)**

a simple faulting mechanism. In the present example, the shear wave velocity, density, and the thickness of the layer are assumed to be of unit magnitude, i.e., $\beta = 1$ m/s, $\rho = 1$ kg/m$^3$, and $h = 1$ m. The parameters of the input field are assumed to be $a = 1$ m, $t_o = 1$ s, $\zeta = 0.2$, and $v_o = 1$ m. Consequently, all the following results can be presented in dimensionless form. The frequency spectrum $V(z, x, \omega)$ is defined by

$$V(x, z, \omega) \equiv |v(x, z, \omega)| = \sqrt{\mathrm{Re}^2(v) + \mathrm{Im}^2(v)} \quad \ldots\ldots\ldots\ldots\ldots\ldots \quad (31)$$

The expansion coefficients $b_{2m-1}$ in Eq. 22 are computed from

$$b_{2m-1} = \frac{8v_o}{(2m-1)\pi}(-1)^m \sin\frac{(2m-1)\pi(\eta-\tau)}{4}\left[\sin\frac{(2m-1)\pi(2-\tau-\eta)}{4}\right];$$

$$m = 1, 2, \ldots, \infty \quad \ldots\ldots\ldots\ldots\ldots\ldots\ldots\ldots\ldots\ldots\ldots\ldots \quad (32)$$

allowing evaluation of the frequency spectra in closed form. Examples of the frequency spectra for shallow source and progressing waves are presented in Fig. 4. For locally standing waves, the spectra are depicted by Fig. 5.

## Rotation

Torsional excitation of structures by horizontally propagating seismic waves is next examined in the simple framework of the model in Fig. 1. The torsional

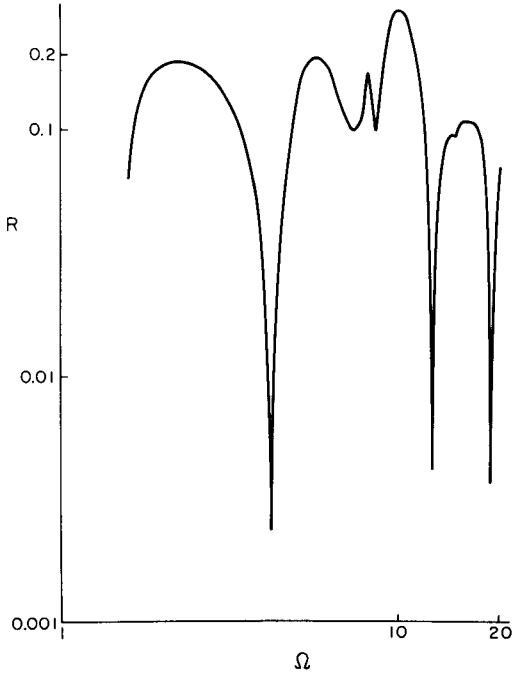


**FIG. 6.—Progressing Waves: Rotation Amplitude Spectrum from Shallow Source ($\tau = 0$, $\eta = 0.2$, $\beta = 1$ m/s, $h = 1$ m)**

component of the rotation field $r_z(x, z, \omega)$ is determined by application of the curl operator to the displacement field $v(x, z, \omega)$. For antiplane-stain model, the $z$-component of the rotation vector represents the torsional excitation. Therefore, it follows from Eq. 22 that

$$r_z(x, z, \omega) = \frac{\partial v}{\partial x} = \frac{F(\omega)}{h} \left\{ i \sum_{m=1}^{n} b_{2m-1} \xi_m \cos \frac{(2m-1)\pi z}{2h} e^{i\xi_m x} - \sum_{m=n+1}^{\infty} b_{2m-1} \left[ \xi_m \cos \frac{(2m-1)\pi z}{2h} e^{-\xi_m x} \right] \right\} e^{-i\omega t} \quad \ldots\ldots\ldots\ldots (33)$$

The rotation amplitude spectrum is then

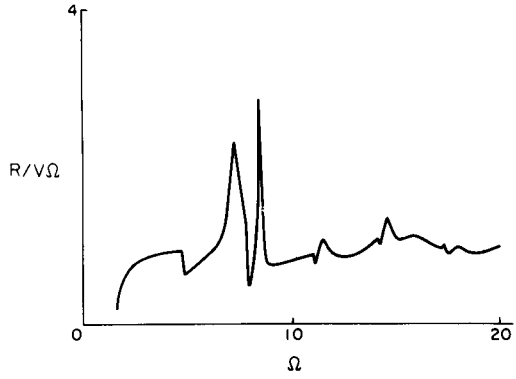


**FIG. 7.—Progressing Waves: Ratio $R/(\Omega V)$ for Shallow Source ($\tau = 0$, $\eta = 0.2$, $\beta = 1$ m/s, $h = 1$ m)**

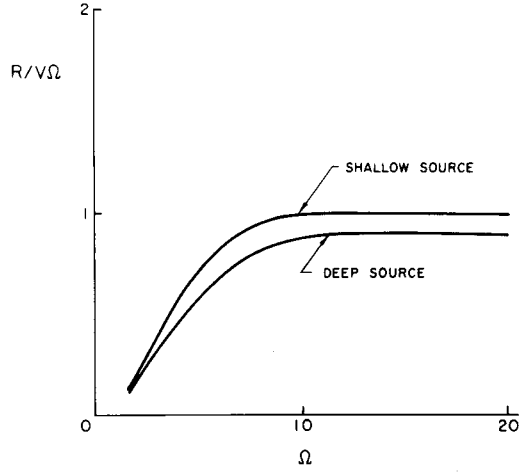


**FIG. 8.—Smoothed Values of $R/(\Omega V)$ for Progressing Waves: Shallow Source ($\tau = 0$, $\eta = 0.2$); Deep Source ($\tau = 0.7$, $\eta = 0.9$)**

$$R(x, z, \omega) = |r_z(x, z, \omega)| = \sqrt{\mathrm{Re}^2(r_z) + \mathrm{Im}^2(r_z)} \quad \ldots\ldots\ldots\ldots\ldots\ldots \quad (34)$$

The result for the $z$-component of the rotation spectrum and progressing waves is exemplified by Fig. 6.

**Rotation Versus Displacement Spectra.**—It is of considerable engineering interest to establish whether there exists a simple relation between the rotation and translation amplitude spectra, since the question of how to calculate the rotation spectra is the displacement spectrum is known often arises.

For the case of a shallow source and progressing waves, the ratio of rotation versus displacement amplitude spectrum $R/(\Omega V)$ is shown in Fig. 7. Examples of spectral ratios $R/(\Omega V)$ smoothed along the dimensionless frequency axis (4) are shown in Fig. 8. It appears from this figure that the ratio of smoothed

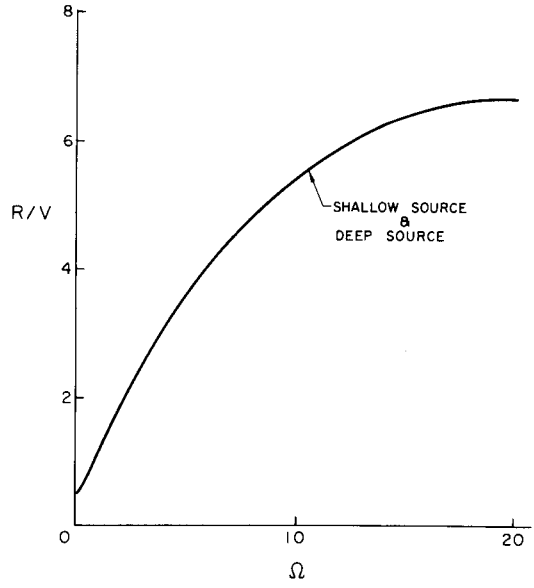


**FIG. 9.—Smoothed Values of $R/V$ for Locally Standing Waves: Shallow Source ($\tau = 0$, $\eta = 0.2$); Deep Source ($\tau = 0.7$, $\eta = 0.9$)**

$R/(\Omega V)$ is nearly constant for a wide frequency range. The results for deep source, depicted by Fig. 8, suggest also small influence of source depth upon this ratio. For shallow (deep) source and locally standing waves, the smoothed $R/V$ spectra are presented in Fig. 9. These results suggest that for certain frequency ranges, one can estimate the rotation spectrum amplitudes in terms of the displacement spectrum amplitude (2) and known $R/V$ ratios.

## Energy Density

Taking into account the geometry of the model and input field, the energy density function at station $x, z$ and at frequency $\omega$ can be defined in the following manner (2)

$$e(x, z, \omega) = \frac{1}{2} \rho \sum_{m=1}^{\infty} \left| b_{2m-1} \cos \frac{(2m-1)\pi z}{2h} e^{i\kappa_m x} \right|^2 \quad \ldots\ldots\ldots\ldots (35)$$

in which $\rho$ = density of the layer. In other words, the total energy density is a sum of energy densities of all modes present at that frequency (locally standing and progressing). For chosen input functions $g$ and $F$, the total energy density is shown by Fig. 10. Since the energy density decreases with increasing $x$, it can be seen from Fig. 10 that the contribution of locally standing waves to the total energy density is of importance for distances $x = 0(h)$ only. For $x/h > 1$, their contribution becomes negligible and the energy density reduces

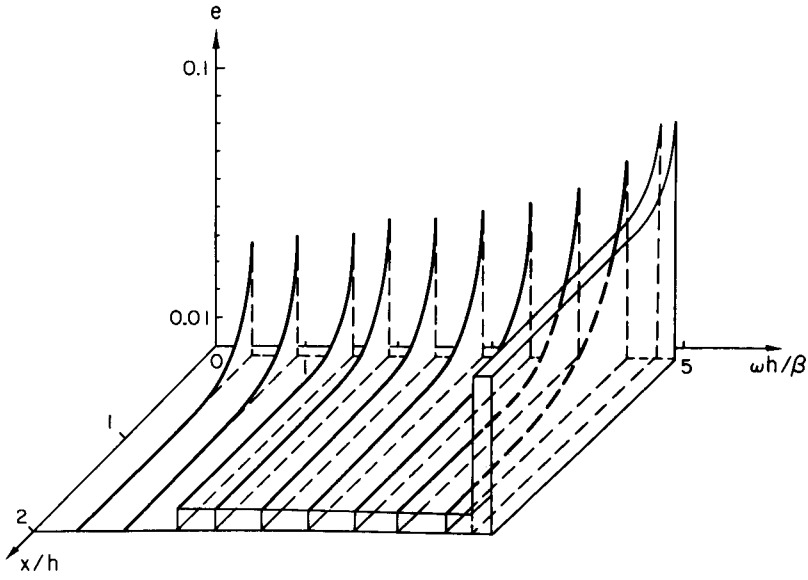


**FIG. 10.—Energy Density for Deep Source ($\tau$ = 0.7, $\eta$ = 0.9, $h$ = 1 m, $\beta$ = 1 m/s, $z$ = 0)**

to that due to progressing waves only. The same conclusion follows for shallow source input as well.

## Conclusions

The exact, steady-state solution has been presented for the response of an elastic layer perfectly bonded upon a rigid half space and subjected to a vertical antiplane type displacement field in such a way as to simulate a simple model of a strike-slip fault. The solution consists of progressing and locally standing waves that decay exponentially with distance from the source.

Detailed comparison of the present analysis with that for the more general multilayered medium (2) reveals that many characteristics of the near field wave propagation are preserved by the simple model of Fig. 1: (1) The average ratio of the spectrum amplitudes of progressing torsional excitation versus the product

of displacement spectrum amplitudes and the frequency, remains constant for a wide range of frequencies; and (2) the contribution of locally standing waves to the total energy density spectrum is significant within a distance which is of the order of the thickness of the layer.

The findings imply that for structures in the immediate vicinity of a strike-slip fault, the contribution of locally standing waves to strong ground shaking must be considered. The foregoing analysis also shows how the torsional excitation can be approximated in terms of the displacement spectrum amplitudes, source depth, and a simple layered model of the medium between the fault and the building site.

## Acknowledgment

The writers express appreciation to Bruce D. Westermo for critical reading of the paper.

## Appendix I.—References

1. Achenbach, J. D., *Wave Propagation in Elastic Solids,* North-Holland Publishing Co., Amsterdam, the Netherlands, 1973.
2. Carrier, G. F., Krook, M., and Pearson, C. E., *Functions of a Complex Variable,* McGraw-Hill Book Co., Inc., New York, N.Y., 1966.
3. Dravinski, M., and Trifunac, M. D., "Static, Dynamic and Rotational Components of Strong Earthquake Shaking Near Faults," *Department of Civil Engineering Report No. CE 79-06,* University of Southern California, Los Angeles, Calif., 1979.
4. Holloway, J. L., Jr., "Smoothing and Filtering of Time Series and Space Fields," *Advances in Geophysics,* Vol. 4, 1958, pp. 351–389.
5. Sneddon, I. M., *The Uses of Integral Transforms,* McGraw-Hill Book Co., Inc., New York, N.Y., 1972.

## Appendix II.—Notation

*The following symbols are used in this paper:*

$a, \tau, \eta, t_o, v_o, \zeta$ = parameters of input functions;
$b_n$ = expansion coefficients;
$e$ = base of natural logarithm;
$e(x, z, \omega)$ = energy density;
$F(\omega)$ = frequency dependent part of input field;
$f^*(n)$ = finite Fourier sine transform of $f(z)$;
$f_1(t), f_2(t)$ = temporal part of input field;
$\tilde{f}(\xi)$ = Fourier sine transform of $f(x)$;
$g(z)$ = spatial part of input field;
$H(\cdot)$ = Heaviside unit step function;
$h$ = thickness of layer;
$\mathrm{Im}(\cdot)$ = imaginary part of $(\cdot)$;
$i$ = $\sqrt{-1}$;
$k$ = wave number;
$n$ = finite Fourier sine transform variable;
$\mathrm{Re}(\cdot)$ = real part of $(\cdot)$;
$t$ = time;

$V$ = frequency spectrum of $v(\omega)$;
$v^i$ = input displacement field;
$\beta$ = shear wave velocity of layer;
$\epsilon$ = element of set;
$\kappa$ = dimensionless wave number;
$\xi$ = Fourier sine transform variable;
$\xi_m$ = poles in complex $\xi$-plane;
$\rho$ = layer density;
$\Omega$ = dimensionless circular frequency; and
$\omega$ = circular frequency.

**Superscripts**

$i$ = input field;
$+$ = value being approached from above;
$*$ = finite Fourier sine transform; and
$\tilde{}$ = Fourier sine transform.

**Subscripts**

$m$ = the $m$th mode.

**15610 RESPONSE TO STRIKE-SLIP VERTICAL FAULT**

KEY WORDS: **Dislocations (materials);** Earthquake engineering; Energy densities; **Faults (geology);** Layers; **Responses; Slip surface;** Steady state

ABSTRACT: Horizontally polarized shear waves in an elastic layer perfectly bonded to a rigid half-space are considered. The layer is subjected to a steady-state horizontal displacement field. The displacement spectrum is evaluated in closed form. It consists of two types of waves: (1)Progressing waves; and (2)locally standing waves. The average ratio of progressing torsional spectra versus the product of the displacement spectra and frequency, remains constant for a wide range of frequencies. The same ratio is strongly frequency-dependent for locally standing waves. The contribution of locally standing waves to displacements is significant for distances from the source which are, at most, an order of one thickness of the layer.

REFERENCE: Dravinski, Marijan, and Trifunac, Mihailo D., "Response of Layer to Strike-Slip Vertical Fault," *Journal of the Engineering Mechanics Division,* ASCE, Vol. 106, No. EM4, **Proc. Paper 15610,** August, 1980, pp. 609-621